NREL National Renewable Energy Laboratory

A national laboratory of the U.S. Department of Energy
Office of Energy Efficiency & Renewable Energy

Innovation for Our Energy Future

Development of Fully Coupled Aeroelastic and Hydrodynamic Models for Offshore Wind Turbines

Preprint

J.M. Jonkman
National Renewable Energy Laboratory

P.D. Sclavounos
Massachusetts Institute of Technology (MIT)

To be presented at the 2006 ASME Wind Energy Symposium
Reno, Nevada
January 10–12, 2006

Conference Paper
NREL/CP-500-39066
January 2006

NREL is operated by Midwest Research Institute • Battelle   Contract No. DE-AC36-99-GO10337

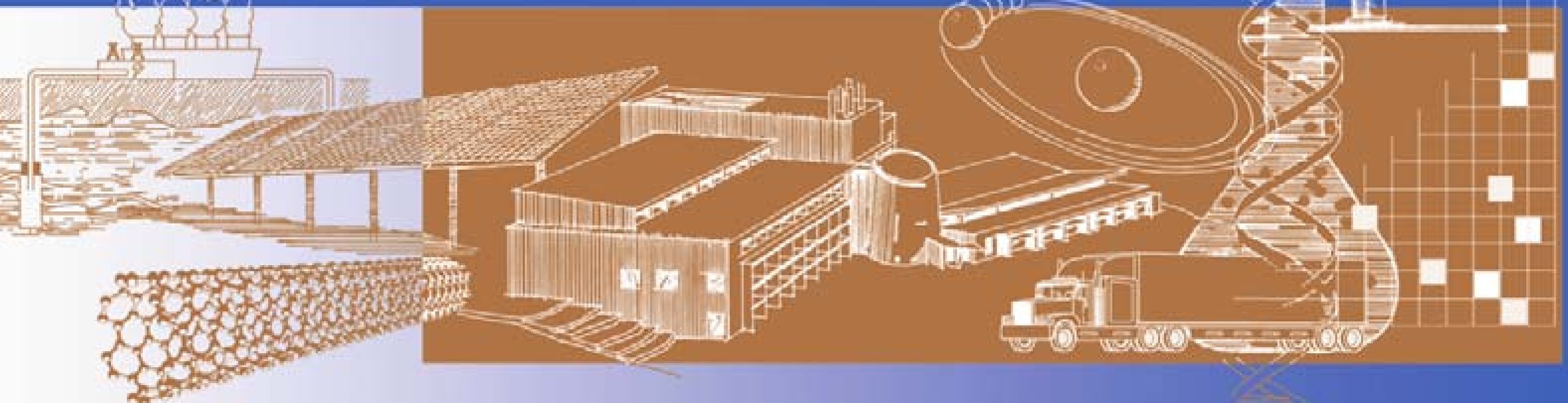

Available electronically at http://www.osti.gov/bridge

Available for a processing fee to U.S. Department of Energy
and its contractors, in paper, from:
U.S. Department of Energy
Office of Scientific and Technical Information
P.O. Box 62
Oak Ridge, TN 37831-0062
phone: 865.576.8401
fax: 865.576.5728
email: mailto:reports@adonis.osti.gov

Available for sale to the public, in paper, from:
U.S. Department of Commerce
National Technical Information Service
5285 Port Royal Road
Springfield, VA 22161
phone: 800.553.6847
fax: 703.605.6900
email: orders@ntis.fedworld.gov
online ordering: http://www.ntis.gov/ordering.htm

Printed on paper containing at least 50% wastepaper, including 20% postconsumer waste

Development of Fully Coupled Aeroelastic and Hydrodynamic Models for Offshore Wind Turbines[*]

Jason M. Jonkman[†]
National Renewable Energy Laboratory (NREL), Golden, Colorado, 80401-3393

and

Dr. Paul D. Sclavounos[‡]
Massachusetts Institute of Technology (MIT), Cambridge, Massachusetts, 02139-4307

Aeroelastic simulation tools are routinely used to design and analyze *onshore* wind turbines, in order to obtain cost effective machines that achieve favorable performance while maintaining structural integrity. These tools employ sophisticated models of wind-inflow; aerodynamic, gravitational, and inertial loading of the rotor, nacelle, and tower; elastic effects within and between components; and mechanical actuation and electrical responses of the generator and of control and protection systems. For *offshore* wind turbines, additional models of the hydrodynamic loading in regular and irregular seas, the dynamic coupling between the support platform motions and wind turbine motions, and the dynamic characterization of mooring systems for compliant floating platforms are also important. Hydrodynamic loading includes contributions from hydrostatics, wave radiation, and wave scattering, including free surface memory effects. The integration of all of these models into comprehensive simulation tools, capable of modeling the fully coupled aeroelastic and hydrodynamic responses of *floating* offshore wind turbines, is presented.

Nomenclature

A	=	amplitude of a regular incident wave
a_i	=	component of the fluid particle acceleration in Morison's equation in the direction of the i^{th} translational degree-of-freedom of the support platform
A_{ij}	=	(i,j) component of the hydrodynamic added mass matrix
A_0	=	waterplane area of the support platform when it is in its undisplaced position
B_{ij}	=	(i,j) component of the hydrodynamic damping matrix
$C_{ij}^{Hydrostatic}$	=	(i,j) component of the linear hydrostatic restoring matrix from waterplane area and the center-of-buoyancy
C_{ij}^{Lines}	=	(i,j) component of the linear restoring matrix from all mooring lines
C_A	=	normalized hydrodynamic added mass coefficient in Morison's equation
C_D	=	normalized viscous drag coefficient in Morison's equation
C_M	=	normalized mass (inertia) coefficient in Morison's equation
D	=	diameter of cylinder in Morison's equation
$dF_i^{Platform}$	=	i^{th} component of the total external load acting on a differential element of cylinder in Morison's

[*] This work has been authored by Midwest Research Institute under Contract No. DE-AC36-99GO10337 with the U.S. Department of Energy. The United States Government retains and the publisher, by accepting the article for publication, acknowledges that the United States Government retains a non- exclusive, paid-up, irrevocable, worldwide license to publish or reproduce the published form of this work, or allow others to do so, for United States Government purposes.
[†] Engineer II-Structural Systems & Dynamics, National Wind Technology Center (NWTC), 1617 Cole Boulevard, AIAA Professional Member.
[‡] Professor, Department of Mechanical Engineering, 77 Massachusetts Avenue.

equation, other than those loads transmitted from the wind turbine and the weight of the support platform

$dF_i^{Viscous}$	=	i^{th} component of the viscous drag load acting on a differential element of cylinder in Morison's equation
dz	=	length of a differential element of cylinder in Morison's equation
f_i	=	component of the forcing function associated with the i^{th} degree-of-freedom
F_i^{Lines}	=	i^{th} component of the total load on the support platform from the contribution of all mooring lines
$F_i^{Lines,0}$	=	i^{th} component of the total mooring line load acting on the support platform in its undisplaced position
$F_i^{Platform}$	=	i^{th} component of the total external load acting on the support platform, other than those loads transmitted from the wind turbine and the weight of the support platform
$F_i^{Viscous}$	=	i^{th} component of the total viscous drag load acting on the support platform from Morison's equation
F_i^{Waves}	=	i^{th} component of the total excitation force on the support platform from incident waves
g	=	gravitational acceleration constant
h	=	water depth
k	=	wavenumber of incident wave
K_{ij}	=	(i,j) component of the wave radiation kernel matrix or impulse response functions of the radiation problem
M_{ij}	=	(i,j) component of the inertia mass matrix
q_j	=	degree-of-freedom j (without the subscript, q represents the set of degrees-of-freedom)
$\dot{q}_j$	=	first time derivative of degree-of-freedom j (without the subscript, $\dot{q}$ represents the set of first time derivatives of the degrees-of-freedom)
$\ddot{q}_j$	=	second time derivative of degree-of-freedom j (without the subscript, $\ddot{q}$ represents the set of first time derivatives of the degrees-of-freedom)
$S_\zeta^{1\text{-}Sided}$	=	one-sided power spectral density of the wave elevation per unit time
$S_\zeta^{2\text{-}Sided}$	=	two-sided power spectral density of the wave elevation per unit time
t	=	simulation time
u	=	set of wind turbine control inputs
v_i	=	component of the fluid particle velocity in Morison's equation in the direction of the i^{th} translational degree-of-freedom of the support platform
V_0	=	displaced volume of fluid when the support platform is in its undisplaced position
W	=	Fourier transform of a realization of a White Gaussian Noise time series process with unit variance
X_i	=	i^{th} component of the complex wave excitation force on the support platform per unit wave amplitude
X,Y,Z	=	set of orthogonal axes making up an original reference frame (when applied to the support platform in particular, X,Y,Z represents the set of orthogonal axes of an inertial reference frame fixed with respect to the mean location of the platform, with the XY-plane designating the still water level and the Z-axis directed upward opposite gravity along the centerline of the undeflected tower when the platform is undisplaced)
x,y,z	=	set of orthogonal axes making up a transformed reference frame (when applied to the support platform in particular, x,y,z represents the set of orthogonal axes of a body-fixed reference frame within the platform, with the xy-plane designating the still water level when the platform is undisplaced and the z-axis directed upward along the centerline of the undeflected tower)
z_{COB}	=	body-fixed vertical location of the center-of-buoyancy of the support platform (relative to the still water level and negative downward along the undeflected tower centerline when the support platform is in its undisplaced position)
β	=	incident wave propagation heading direction
δ_{ij}	=	(i,j) component of the Kronecker-Delta function (i.e., identity matrix), equal to unity when $i = j$ and zero when $i \neq j$
ζ	=	instantaneous elevation of incident waves
$\theta_1,\theta_2,\theta_3$	=	set of orthogonal rotations used to convert from an original to a transformed reference frame (when applied to the support platform in particular, $\theta_1,\theta_2,\theta_3$ represent the roll, pitch and yaw rotations of the platform about the axes of the inertial reference frame)

ρ = water density
σ_{ζ}^{2} = variance of the instantaneous elevation of incident waves
τ = dummy variable with the same units as the simulation time
ω = frequency of incident wave or frequency of oscillation of a particular mode of motion of the platform

I. Introduction

DESIGNERS of onshore wind turbines rely extensively on the use of comprehensive aeroelastic simulators, also known as design codes, to efficiently design and analyze wind turbines, in order to obtain cost effective machines that achieve favorable performance while maintaining structural integrity. These aeroelastic tools used to design *onshore* wind turbines are comprehensive in nature, employing sophisticated models of turbulent and deterministic wind-inflow; aerodynamic, gravitational, and inertial loading of the rotor, nacelle, and tower; elastic effects within and between components and in the foundation; and mechanical actuation and electrical responses of the generator and of control and protection systems.

In the *offshore* environment, additional loading is present, and additional dynamic behavior must be considered. Wave-induced forcing is the most apparent new source of loading, and it imparts new and difficult challenges for wind turbine analysts. Additional offshore loads arise from the impact of floating debris or ice and from marine growth buildup on the substructure. The analysis of offshore wind turbines must also account for the dynamic coupling between the support platform motions and turbine motions, as well as the dynamic characterization of the mooring system for compliant floating platforms.

This work is focused on the development of comprehensive simulation tools that are capable of modeling the fully coupled aeroelastic and hydrodynamic responses of *floating* offshore wind turbines, as opposed to wind turbines with fixed-bottom support structures. We place our emphasis on floating offshore wind turbine support platforms because worldwide the *deepwater* (> 30m) wind resource has been shown to be extremely abundant, with the U.S. potential ranked second only to China, and because floating platforms may be the most economical means of deploying offshore wind turbines at these sites. (The current practice for fixed-bottom offshore wind turbines of driving monopiles into the seabed or relying on conventional concrete gravity bases becomes economically infeasible at these depths.) For instance, the wind resource potential between 5 and 50 nautical miles off the coast of the U.S., most of which is deepwater, is estimated to be more than the total currently installed electrical generating capacity of the U.S. (over 900,000 MW). Much of this potential lies close to major coastal urban populations.

Over the past decade, the U.S. Department of Energy's (DOE's) National Renewable Energy Laboratory (NREL)[§] has sponsored the development, verification, and validation of comprehensive aeroelastic simulators capable of predicting both the extreme and fatigue loads of *onshore* horizontal-axis wind turbines (HAWTs). FAST (Fatigue, Aerodynamics, Structures, and Turbulence) and MSC.ADAMS® (Automatic Dynamic Analysis of Mechanical Systems) ("ADAMS" is used to imply "MSC.ADAMS®" throughout this paper)[4,5] are two of the primary design codes used by the U.S. wind industry and are the two most promoted by NREL's National Wind Technology Center (NWTC)[**]. FAST is a publicly-available code of medium complexity for determining the structural response of HAWTs. It is written and distributed by the NWTC. The code is based on previous developments done at Oregon State University and the University of Utah. The more complex ADAMS code is a commercially available, general purpose, multibody-dynamics code from MSC.Software Corporation[††] that is adaptable for modeling wind turbines. Both FAST and ADAMS use the AeroDyn aerodynamic subroutine package developed by Windward Engineering LLC[‡‡] for calculating aerodynamic forces.

In order to adapt these design codes so that they are useful in the analysis of *offshore* wind turbines, it is beneficial to garner the design philosophies and computational methodologies employed by the offshore oil and gas industries. The Center for Ocean Engineering at the Massachusetts Institute of Technology (MIT)[§§] has sponsored the development, verification, and validation of comprehensive hydrodynamic computer programs capable of analyzing the wave interaction and dynamic responses of offshore platforms in both the frequency and time domains. SWIM-MOTION-LINES (SML)[7-10] from MIT is a publicly-available suite of computer modules for determining the hydrodynamic properties and responses of floating structures operating in wind, waves, and current in waters of moderate to large depth. The SWIM module analytically solves the linear- and second-order frequency

[§] Website: http://www.nrel.gov/.
[**] Website: http://www.nrel.gov/wind/.
[††] Website: http://www.mscsoftware.com/.
[‡‡] Website: http://www.windwardengineering.com/.
[§§] Website: http://oe.mit.edu/page.php?name=index.

domain hydrodynamic problems for platforms composed of simple geometry, such as arrays of vertical, surface-piercing cylinders. The MOTION module finds solutions of the large amplitude time domain slow-drift responses and the LINES module determines the nonlinear mooring line / tether / riser effects upon the platform. The computer program WAMIT® (Wave Analysis at MIT), a commercially available product from WAMIT, Inc.[***], solves the wave interaction problem for bodies of complex geometry using the numerical panel method technique.

Because the upcoming international design standard for offshore wind turbines requires that an integrated loads analysis be performed when certifying a machine, it is important to develop comprehensive simulation tools that are capable of modeling the fully coupled aeroelastic and hydrodynamic responses of floating offshore wind turbines. The NREL-sponsored study by Concept Marine Associates (CMA) on the design of a semi-submersible platform and anchor foundation system for wind turbine support also recommended the development of such a simulation tool. Design optimization would also be impossible without taking into account the fully coupled response.

The fully coupled simulation tools must be general enough to allow us to analyze a variety of support platform configurations. The reason for this generality is that numerous platform configurations are possible when one considers the variety of mooring systems, tanks, and ballast options that are utilized in the offshore oil and gas industries, but little work has been performed to determine the technical and economic feasibility of any of the concepts when applied to offshore wind turbines. Figure 1 illustrates several of the concepts, classified in terms of how the designs achieve static stability. The Spar-buoy concept achieves stability by using ballast to lower the center-of-gravity (COG) below the center-of-buoyancy (COB) and can be moored by catenary or taut lines. The Tension Leg Platform (TLP) achieves stability through the use of mooring line tension brought about by excess buoyancy in the tank. The barge concept achieves stability through waterplane area and is generally moored by catenary lines. Hybrid concepts, using features from all three classes, are also an option.

The fully coupled simulation tools must also be based in the *time domain*. Even though frequency domain analyses are commonly employed in the offshore oil and gas industries, the detailed design stage analyses of wind turbines must take place in the time domain in order to capture the nonlinear dynamic characteristics and transient

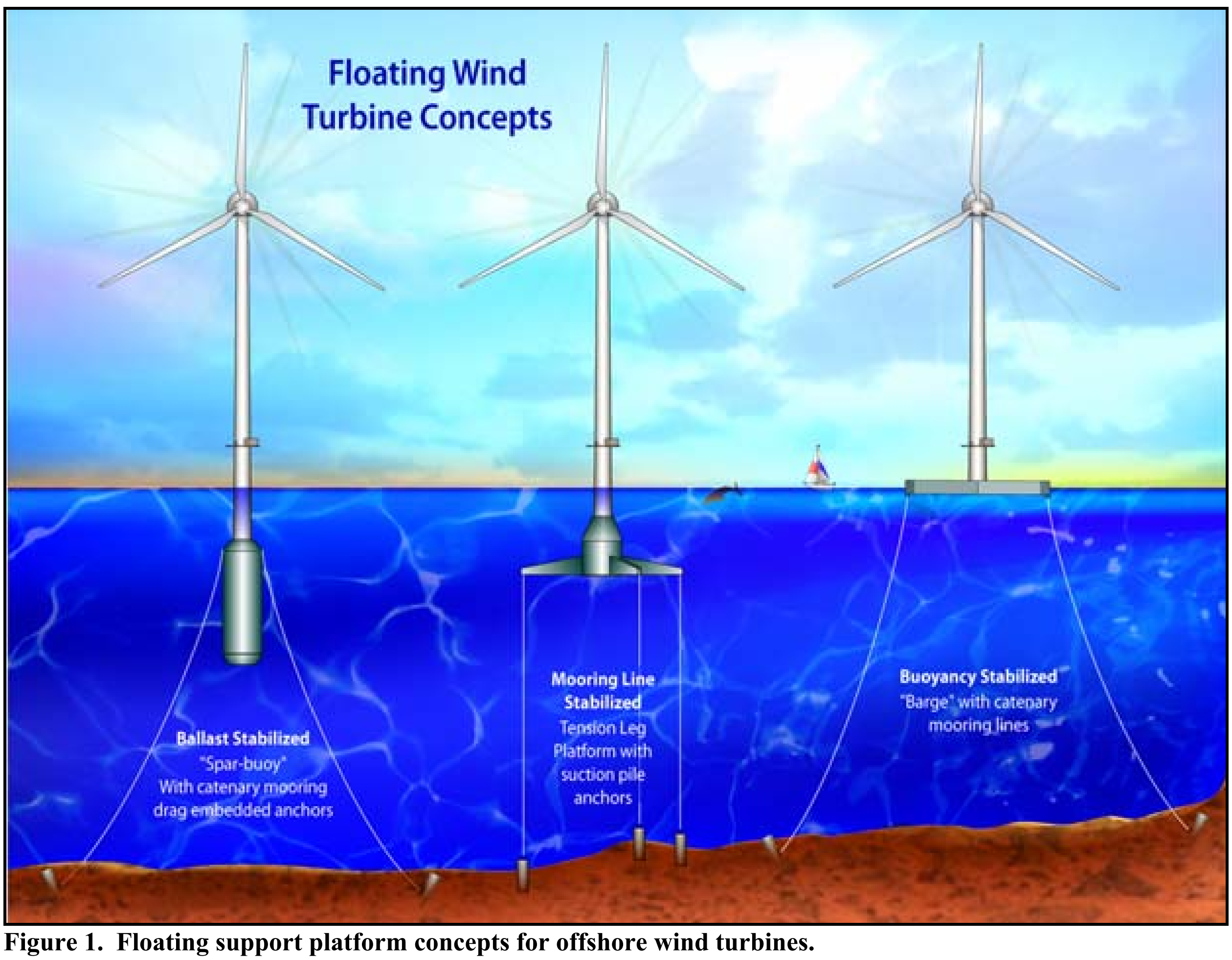

Figure 1. Floating support platform concepts for offshore wind turbines.

events important to wind turbines.

This paper presents the results of an effort to upgrade FAST to include the additional loading and responses representative of floating offshore wind turbines. Additionally, enhancements to FAST's ADAMS preprocessor make it easy to assemble a more comprehensive ADAMS model of a floating offshore wind turbine using the configuration inputs available in FAST. The utilization of the SML and WAMIT codes in the overall solution is discussed.

The contents of this paper relate to the addition of support platform kinematics and kinetics, the incorporation of support platform hydrodynamic loading, and the inclusion of mooring system dynamics. Numerical results will be presented in a future paper. We make extensive use of equations to describe the hydrodynamic formulations as they relate to floating offshore wind turbines. For conciseness, the derivations of these equations are not included; it is the form of the equations and the physics behind them that we want to emphasize. (For the derivations, please refer to the associated references.) Nevertheless, at first glance, the extensive use of equations might appear a bit formidable to the casual reader. So why include this complexity? First, the approach we have taken to implement hydrodynamic loading into our aeroelastic simulators is substantially different than the approach taken by other simulation specialists who have analyzed fixed-bottom offshore wind turbine support structures.[14,16-20] Our approach is also more comprehensive than the approach used by others who have performed preliminary dynamic analyses of floating wind turbines.[13,21-24] These dissimilarities will be discussed at greater length later in the paper. Second, it is very beneficial for those readers who have technical knowledge of wind turbine modeling, but are unfamiliar with the offshore side of the business, to overview the technical issues involved when diving into the area of offshore wind energy simulation.

Before describing the additional formulations needed for upgrading the simulators to handle offshore dynamic responses, it is constructive to step back and outline the general class of modeling theories employed by the above-water (wind turbine) portions of FAST, ADAMS, and AeroDyn. This is discussed in the following section. The assumptions inherent in the below-water (support platform) portions of the simulators are discussed in section IB.

A. General Overview of Aeroelastic Modeling with FAST, ADAMS, and AeroDyn

The FAST model employs a combined modal and multibody dynamics formulation. Flexibility in the blades and tower are characterized using a linear modal representation that assumes small deflections. The flexibility characteristics of these members are determined by specifying distributed stiffness and mass properties along the span of the members, and by prescribing their mode shapes through equivalent polynomial coefficients. FAST allows for two flapwise and one edgewise bending mode per blade and two fore-aft and two side-to-side bending modes in the tower. Torsional flexibility in the drivetrain is modeled using an equivalent linear spring and damper model in the low-speed shaft. The nacelle and hub are modeled in FAST as rigid bodies with appropriate mass and inertia terms. Time marching of the nonlinear equations of motion is performed using a constant-time-step, Adams-Bashforth-Adams-Moulton, predictor-corrector integration scheme. FAST has a limited number of structural degrees-of-freedom (DOFs) but can model most common wind turbine configurations and control scenarios. These DOFs can be enabled or locked through switches, permitting the user to easily increase or decrease the fidelity of the model. All but the blade and tower DOFs may exhibit large displacements without loss of accuracy.

FAST can extract linearized representations of the complete nonlinear aeroelastic wind turbine model. This analysis capability is useful for developing state matrices of a wind turbine "plant" to aid in controls design and analysis. It is also useful for determining the full system modes of an operating or stationary HAWT through the use of a simple eigenanalysis.

Another feature available in FAST is the ADAMS preprocessor. The FAST-to-ADAMS preprocessor uses the configuration information available in the FAST input files to construct an ADAMS dataset (model) of the complete aeroelastic wind turbine.

The structural dynamics model of ADAMS is more sophisticated than the one in FAST, permitting an almost unlimited combination of configurations and DOFs. It is not a wind turbine-specific code and is routinely used by members of the automotive, aerospace, and robotics industries. Flexible members, such as the blades and tower of a wind turbine are modeled in ADAMS using a series of lumped masses connected by flexible "fields" akin to multidimensional spring dampers. ADAMS can model the drivetrain through a similar series of lumped masses and flexible fields, or through a simple, single-DOF hinge/spring/damper element. As in FAST, the nacelle and hub are typically modeled using rigid bodies with lumped mass and inertia properties. ADAMS incorporates a similar time-marching scheme as the one in FAST, except that the ADAMS scheme incorporates a variable time step algorithm.

It is often necessary to use the more complicated ADAMS code in place of FAST since ADAMS has many features that FAST does not. These include torsional and extensional DOFs in the blades and tower, flap/twist coupling in the blades, mass and elastic offsets in the blades, mass offsets in the tower, actuator dynamics in the blade pitch controller, etc. It is also advantageous to use ADAMS to verify the dynamic responses obtained from FAST when we add new DOFs to FAST. This is because the dynamics in ADAMS are not defined by the user and are well verified.

Both FAST and ADAMS use the AeroDyn aerodynamic subroutine package for computing aerodynamic forces. This aerodynamic package models rotor aerodynamics using the classic, equilibrium-based, blade-element/momentum (BEM) theory or by using a generalized dynamic inflow model, both of which include the effects of axial and tangential induction. The BEM model uses tip and hub losses as characterized by Prandtl. Dynamic-stall behavior can be characterized using the optional Beddoes-Leishman dynamic stall model. The element motion and position are included in the calculation of the instantaneous relative wind vector at each blade element, making the codes fully aeroelastic. More details can be found in the AeroDyn Theory Manual.

B. Model Development Assumptions for the Support Platform

We have invoked a number of assumptions, in addition to those previously inherent with the aeroelastic simulators, when adding support platform kinematics, kinetics, hydrodynamic loading, and mooring system dynamics.

With regards to the support platform kinematics and kinetics, we assume that the support platform is a six DOF rigid body whose three rotational displacements are *small*. The implications of this assumption are not deemed to be critical, as discussed in section II. Additionally, the tower is assumed to be perpendicularly cantilevered to the support platform. The inertia (not including the wind turbine) and COB of the support platform are also assumed to lie on the centerline of the undeflected tower.

With regards to the mooring system dynamics, we assume that the mooring lines do not have bending stiffness.

The fundamental assumption of this work is *linearization of the hydrodynamics problem*. The assumption of linearity in the field of marine hydrodynamics signifies many things.

First, linearization of the hydrodynamics problem implies that the *wave amplitudes are much smaller than the wavelengths*. This allows us to use the simplest wave kinematics theory known as *Airy wave theory*. This necessarily precludes us from being able to model steep or breaking waves and the resulting nonlinear wave-induced "slap" and "slam" loading. This is a reasonable assumption for most waves in deep water and for small amplitude waves in shallow water. However, when waves become large or propagate towards shore in shallow water, higher order wave kinematics theories are required.

Second, linearization of the hydrodynamics problem implies that the *translational displacements of the support platform are small relative to the size of the body* (i.e., characteristic body length). In this way, the hydrodynamics problem can be split into separate and simpler problems: a radiation problem, a scattering problem, and a hydrostatics problem. We will discuss the details of these in section III. As is often misunderstood, linearity of the hydrodynamics problem does not imply that the characteristic length of the support platform needs to be small relative to the wavelength of the waves. When this *is* the case, the hydrodynamic diffraction problem (part of the scattering problem) can be greatly simplified; however, we do not invoke this simplification in the present analysis.

Third, linearization of the hydrodynamics problem suggests that we can take advantage of the powerful technique of *superposition*. We will discuss how superposition relates to the hydrodynamics problem in section III.

Naturally, linearization of the hydrodynamics problem implies that second- or higher-order hydrodynamic effects are not accounted for in the model. Though this follows from the definition of linear, it is important to discuss what it signifies. Second- or higher-order nonlinear hydrodynamic loading models more properly account for the loading about the instantaneous wetted surface and are required when the support platform motions are large relative to their characteristic lengths. Slow-drift excitation, resulting from difference-frequency effects from multiple incident waves, are neglected in the linear hydrodynamics problem. They are important for wave-induced loading on support platforms with small draft, large waterplane area, and mooring system configurations that impose little resistance to surge and sway, such as barge designs with catenary mooring lines. Sum-frequency effects from multiple incident waves are also neglected in the linear hydrodynamics problem, but are important for analyzing "ringing" behavior in support platforms with mooring systems that impose a strong resistance to heave, such as TLP designs.

Another assumption we make is that there is *no sea current*. We invoke this assumption more to simplify the radiation problem, which is complicated by sea current or forward speed effects, rather than out of necessity. Just like the wind-induced thrust loading on the wind turbine rotor, sea currents bring about a mean offset of the support platform relative to the undisplaced position. For compliant floating systems, the mooring system resistance is often a highly nonlinear function of displacement; thus, the effects of sea currents on mooring system resistance may be important for some designs. Ignoring sea currents also prohibits us from including the effects of vortex-induced vibrations (VIV). When the VIV frequency nears a natural frequency of the system, a resonance phenomenon known as lock-in may occur. VIV is also known to be critical for the stability of some designs.

Finally, we *ignore the potential loading from floating debris or sea ice*. Sea ice can be a significant source of loading if the support platform is intended to be used in areas in which sea ice is present. Around the continental United States, this may be of particular concern when designing offshore wind turbine support platforms for the Great Lakes.

Please also note that the classical marine hydrodynamics problem takes advantage of unsteady, potential flow theory to derive the governing equations of fluid motion. This theory assumes the fluid is *incompressible, inviscid, and subject only to conservative body forces* (i.e., gravity) and that the flow is *irrotational*.

II. Support Platform Kinematics and Kinetics

The first step necessary for upgrading existing onshore wind turbine analysis tools so that they are useful in the design of offshore units is to introduce DOFs needed to describe the motion of the support platform. For floating systems, it is crucial that all six rigid-body modes of motion of the support platform be included in the development. These include translational surge, sway, and heave DOFs and rotational roll, pitch, and yaw DOFs as shown in Fig. 2. In this figure, X,Y,Z represents the set of orthogonal axes of an inertial reference frame fixed with respect to the mean location of the support platform, with the XY-plane designating the still water level (SWL) and the Z-axis directed upward opposite gravity along the centerline of the undeflected tower when the support platform is undisplaced.

One may question whether the support platform yaw DOF is necessary in light of the fact that most of the support platforms that have been proposed for floating wind turbines are more or less axisymmetric, and there is no hydrodynamic mechanism that will induce yaw moments on such bodies. However, yaw moments are induced by the wind turbine. These are primarily the result of (1) the aerodynamic loads on the rotor when a yaw error exists between the rotor axis and nominal wind direction, and (2) the spinning inertia of the rotor combined with pitching motion, which induce a gyroscopic yaw moment.

As implied by item (2) in the previous paragraph, the dynamic coupling between the motions of the support platform and the wind turbine are crucial in the development of the equations of motion. In fact, the term "fully coupled" in the title of this paper is used to imply that the wind turbine's response to wind and wave excitation is fully coupled *through* the structural dynamic response. It does not imply that the wind inflow and sea state need to be correlated. We are not attempting to model the air/sea interface, which is a very complicated multiphase fluid-flow problem!

We obtain all of the dynamic couplings between the motions of the support platform and the wind turbine by incorporating all appropriate DOFs in the derivations of the kinematics expressions for the points and reference frames in the system. For example, before the addition of the six rigid-body support platform DOFs, the kinematics expressions for the position, velocity, and acceleration vectors of a point in the nacelle depended only on the tower mode and nacelle yaw DOFs because the tower base reference frame was the inertial frame. With the addition of the six rigid-body support platform DOFs, the tower base reference frame now moves with the support platform, and thus, the kinematics expressions for a point in the nacelle now also depend on the support platform DOFs. Indeed, the kinematics expressions for all of the points and reference frames in the system are now affected by support platform DOFs.

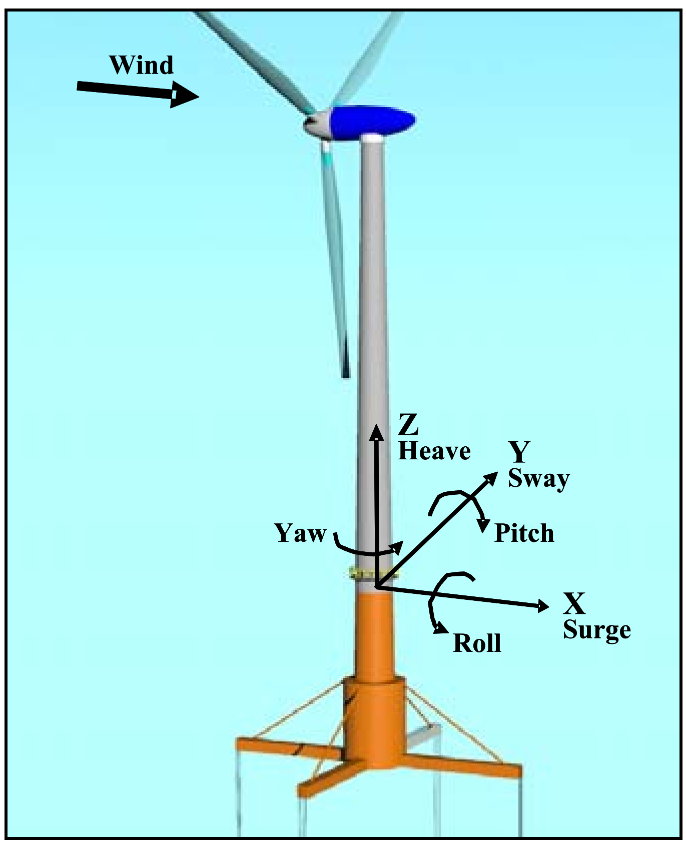

Figure 2. Support platform degrees-of-freedom.

With the assumption that all rotations of the support platform are small, rotation sequence is unimportant and we can avoid all of the complications involved with deriving and implementing the equations of motion by means of Euler angles, where the order of rotation is significant. If x,y,z are the axes of the reference frame resulting from a transformation involving three orthogonal rotations (θ_1,θ_2,θ_3) about the axes of an original reference frame X,Y,Z, then by making use of the small angle approximations for sine and cosine, the standard Euler angle transformation relating the original and transformed reference frames simplifies to:

$$\begin{Bmatrix} x \\ y \\ z \end{Bmatrix} \approx \begin{bmatrix} 1 & \theta_3 & -\theta_2 \\ -\theta_3 & 1 & \theta_1 \\ \theta_2 & -\theta_1 & 1 \end{bmatrix} \begin{Bmatrix} X \\ Y \\ Z \end{Bmatrix}. \tag{1}$$

The approximation sign (≈) in Eq. (1) is used in place of an equals symbol (=) since the transformation matrix loses its orthonormal attribute when making use of the small angle approximations. This implies that the transformed reference frame is not made up of a set of mutually orthogonal axes. (All transformation matrices relating sets of mutually orthogonal axes must be orthonormal.) Because the use of axes that are not mutually orthogonal leads to inaccuracies that propagate in the dynamic response calculations, we invoke a correction to the transformation matrix in Eq. (1) to ensure that it remains orthonormal. From matrix theory we know that the closest orthonormal matrix to a given matrix, in the Frobenius norm sense, is $[\mathrm{U}][\mathrm{V}]^T$ where [U] and [V] are the matrices of eigenvectors inherent in the Singular Value Decomposition (SVD) of the given matrix and ^{T} represents a matrix transpose. By performing these operations, the correct transformation expression is found to be:

$$\begin{Bmatrix} x \\ y \\ z \end{Bmatrix} = \begin{bmatrix} \dfrac{\theta_1^2\sqrt{1+\theta_1^2+\theta_2^2+\theta_3^2}+\theta_2^2+\theta_3^2}{\left(\theta_1^2+\theta_2^2+\theta_3^2\right)\sqrt{1+\theta_1^2+\theta_2^2+\theta_3^2}} & \dfrac{\theta_3\left(\theta_1^2+\theta_2^2+\theta_3^2\right)+\theta_1\theta_2\left(\sqrt{1+\theta_1^2+\theta_2^2+\theta_3^2}-1\right)}{\left(\theta_1^2+\theta_2^2+\theta_3^2\right)\sqrt{1+\theta_1^2+\theta_2^2+\theta_3^2}} & \dfrac{-\theta_2\left(\theta_1^2+\theta_2^2+\theta_3^2\right)+\theta_1\theta_3\left(\sqrt{1+\theta_1^2+\theta_2^2+\theta_3^2}-1\right)}{\left(\theta_1^2+\theta_2^2+\theta_3^2\right)\sqrt{1+\theta_1^2+\theta_2^2+\theta_3^2}} \\ \dfrac{-\theta_3\left(\theta_1^2+\theta_2^2+\theta_3^2\right)+\theta_1\theta_2\left(\sqrt{1+\theta_1^2+\theta_2^2+\theta_3^2}-1\right)}{\left(\theta_1^2+\theta_2^2+\theta_3^2\right)\sqrt{1+\theta_1^2+\theta_2^2+\theta_3^2}} & \dfrac{\theta_1^2+\theta_2^2\sqrt{1+\theta_1^2+\theta_2^2+\theta_3^2}+\theta_3^2}{\left(\theta_1^2+\theta_2^2+\theta_3^2\right)\sqrt{1+\theta_1^2+\theta_2^2+\theta_3^2}} & \dfrac{\theta_1\left(\theta_1^2+\theta_2^2+\theta_3^2\right)+\theta_2\theta_3\left(\sqrt{1+\theta_1^2+\theta_2^2+\theta_3^2}-1\right)}{\left(\theta_1^2+\theta_2^2+\theta_3^2\right)\sqrt{1+\theta_1^2+\theta_2^2+\theta_3^2}} \\ \dfrac{\theta_2\left(\theta_1^2+\theta_2^2+\theta_3^2\right)+\theta_1\theta_3\left(\sqrt{1+\theta_1^2+\theta_2^2+\theta_3^2}-1\right)}{\left(\theta_1^2+\theta_2^2+\theta_3^2\right)\sqrt{1+\theta_1^2+\theta_2^2+\theta_3^2}} & \dfrac{-\theta_1\left(\theta_1^2+\theta_2^2+\theta_3^2\right)+\theta_2\theta_3\left(\sqrt{1+\theta_1^2+\theta_2^2+\theta_3^2}-1\right)}{\left(\theta_1^2+\theta_2^2+\theta_3^2\right)\sqrt{1+\theta_1^2+\theta_2^2+\theta_3^2}} & \dfrac{\theta_1^2+\theta_2^2+\theta_3^2\sqrt{1+\theta_1^2+\theta_2^2+\theta_3^2}}{\left(\theta_1^2+\theta_2^2+\theta_3^2\right)\sqrt{1+\theta_1^2+\theta_2^2+\theta_3^2}} \end{bmatrix} \begin{Bmatrix} X \\ Y \\ Z \end{Bmatrix}. \tag{2}$$

It is a trivial exercise to show that the transformation matrix in Eq. (2) is orthonormal. When applied to the support platform, x,y,z represents the set of orthogonal axes of the body-fixed reference frame within the support platform and θ_1,θ_2,θ_3 are the roll, pitch and yaw rotations of the support platform about the axes of the inertial reference frame X,Y,Z. Similar labeling is used when applying Eq. (2) to relate a reference frame that is oriented with an element of a deflected blade (or tower) to the reference frame fixed in the root of the blade (or tower)—in this case the rotations are the flap, lag, and twist slopes of the blade (or tower) element.

In FAST, we have implemented Eq. (2) instead of Eq. (1) for all transformations relating the support platform to the inertial frame, for all transformations relating the deflected tower elements to the tower base, and for all transformations relating the deflected blade elements to the root of the blade. Though not shown here, we have demonstrated that incorporating Eq. (2) in FAST rather than Eq. (1) leads to dynamic responses that are in much better agreement to responses obtained from ADAMS, which uses Euler angles, especially as the magnitude of the angles increases. The dynamic responses are more accurate when Eq. (2) is used in place of Eq. (1) since such transformation matrices get multiplied in series when determining the orientation of subsystems far along the load path away from the inertia frame, such as in a tower or blade element. And thus, errors in a single transformation matrix are compounded when multiplied together. If the wind turbine were very rigid, the correction would not be necessary.

The transformation expression of Eq. (2) still loses considerable accuracy when the angles greatly exceed 15°, but this upper-bound should be adequate for wind turbine support platform designs. This is because (1) the platform must be stable enough to allow access for maintenance personnel, and (2) the energy capture from the wind is proportional to the swept area of the rotor disk normal to the wind direction, which greatly diminishes with increasing angular displacement of the support platform (especially in pitch).

The equations of motion in FAST are derived and implemented using Kane's dynamics. Though it is a long and tedious process, there is no particular difficulty in the derivation, which will not be presented here. It involves first deriving kinematics expressions for the position, velocity, and acceleration vectors for all of the points and reference frames in the system, taking into account all appropriate DOFs as described above. This is manageable when expressing terms relative to an appropriate reference frame, taking advantage of transformation relationships like Eq. (2). For example, with the tower assumed to be cantilevered to the support platform, it is fairly simple to write the expression for the angular velocity of a tower element relative to the support platform; the absolute angular velocity of the tower element is then just the vector sum of the angular velocity relative to the support platform and the angular velocity of the support platform relative to the inertia frame. The angular velocity of the support platform relative to the inertia frame is just the vector sum of the first time derivatives of the roll, pitch, and yaw DOFs.

Once the kinematics expressions are derived, the partial velocity vectors utilized by Kane's dynamics may be established. These, along with expressions for the generalized active and inertia forces, establish the kinetics and lead systematically to the complete, nonlinear equations of motion of the fully coupled wind turbine and support platform.

The kinetics expressions for the support platform include contributions from platform inertia, gravity, hydrodynamics, and the mooring system. The implementation we employ assumes that the inertia of the support platform (not including the wind turbine) lies on the centerline of the undeflected tower; a point mass and all three principal inertias of the support platform (roll, pitch, and yaw) are included in this model. The effects of marine growth buildup on the support platform can be incorporated through a suitable adjustment of the platform mass and inertia.

Once derived, the complete, nonlinear equations of motion of the fully coupled wind turbine and support platform are of the general form:

$$M_{ij}\left(q,u,t\right)\ddot{q}_j = f_i\left(q,\dot{q},u,t\right), \tag{3}$$

where M_{ij} is the (i,j) component of the inertia mass matrix, which depends nonlinearly on the set of DOFs (q), control inputs (u), and time (t), $\ddot{q}_j$ is the second time derivative of DOF j, and f_i is the component of the forcing function associated with DOF i, which depends nonlinearly on the set of DOFs and their first time derivatives (q and $\dot{q}$), as well as the set of control inputs and time (u and t), and is positive in the direction of positive motion of DOF i. We are employing Einstein notation here, where it is implied that when a subscript variable appears twice in a single term, we are summing over all of its possible values. In FAST, for example, subscripts i and j range from one to the total number of DOFs in the model (22 for a two-bladed floating wind turbine or 24 for a three-bladed floating wind turbine).

Naturally, when hydrodynamic loading is present on the support platform, hydrodynamic impedance forces, including the effects of added mass and damping, are important. The *added mass* components of these forces are present because the density of water is of the same order of magnitude as the density of the materials that make up the primary structure. This is in contrast to aerodynamic loading on the wind turbine, which can ignore the effects of added mass, since the density of air is much less than the density of the materials that make up the primary structure. Thus, in order to ensure that the equations of motion are not implicit (that is, we want to avoid f_i depending on $\ddot{q}$), the total external load acting on the support platform, other than those loads transmitted from the wind turbine and the weight of the support platform, must be split into two components, an added mass component summing with M_{ij} and the rest of the load adding to f_i. That is, the total external load on the support platform, $F_i^{Platform}$, must be written as follows:

$$F_i^{Platform} = -A_{ij}\ddot{q}_j + f_i, \tag{4}$$

where A_{ij} is the (i,j) component of the impulsive hydrodynamic added mass matrix to be summed with M_{ij} and f_i is the i^{th} component of the external support platform load associated with everything but A_{ij}, which will be included with the rest of the forcing function in Eq. (3). In Eq. (4), subscripts i and j range from one to six; one for each support platform DOF (*1* = surge, *2* = sway, *3* = heave, *4* = roll, *5* = pitch, *6* = yaw). The forms of these added mass and forcing function terms are discussed in section III.

Our implementation of the kinetics is not specific to the dynamic response of offshore floating systems, but can be used as the basis for modeling onshore foundations and fixed-bottom offshore foundations as well. In the case of fixed-bottom offshore foundations, the contribution to the kinetics expressions from the mooring system is replaced with contributions from soil added mass, elasticity, and damping. In the case of onshore foundations, the effects of hydrodynamic loading are obviously ignored.

III. Support Platform Hydrodynamic Loading

Hydrodynamic loading is included within computer simulations by incorporating a suitable combination of wave kinematics and wave loading models in regular and irregular seas. Time domain hydrodynamic theories are used to relate simulated ambient wave elevation records to loads on the platform. Hydrodynamic loads result from the integration of the dynamic pressure of the water over the wetted surface of the support platform and include contributions from inertia (added mass) and linear drag (radiation), buoyancy (restoring), incident wave scattering (diffraction), current, and nonlinear effects.

We discuss the true linear hydrodynamic loading equations in the time domain next by taking advantage of the assumptions outlined in section IB. By *true* hydrodynamic loading equations, we mean that these equations satisfy the linearized governing boundary value problems (BVPs) *exactly* without restriction on platform size, shape, or manner of motion (other than those required for the linearization assumption to hold). The true linear hydrodynamic loading equations in the time domain are the equations we have implemented in FAST and ADAMS. These are compared and contrasted with alternative hydrodynamic formulations in section IIIB. The *alternative* hydrodynamic formulations are routinely used in the offshore industry but contain restrictions that limit their applicability in the analysis of floating offshore wind turbines.

A. The True Linear Hydrodynamic Loading Equations in the Time Domain

In linear hydrodynamics, the problem can be split into three simpler problems: a radiation problem, a scattering problem, and a hydrostatics problem.[29,30] The *radiation* problem seeks to find the loads on the support platform when the body is forced to oscillate in its various modes of motion when there are *no incident waves present*. The resulting loads are brought about as the body *radiates* waves away from itself (i.e., generates outgoing waves) and include contributions from added mass and wave radiation damping. The *scattering* problem seeks to find the loads on the support platform when the *body is fixed at its mean position* (no motion!) and incident waves are present and *scattered* by the body. The loads are the result of the undisturbed pressure field (Froude-Kriloff) and wave diffraction. The *hydrostatics* problem is elementary, but is nevertheless crucial in the overall behavior of the floating wind turbine.

In section II, we showed that the total external load on the support platform, other than those loads transmitted from the wind turbine, is in the form of Eq. (4). In the true linear hydrodynamics problem, f_i in Eq. (4) is of the form shown in Eq. (5).[31,32] The second term in Eq. (5), F_i^{Lines}, represents the total load on the support platform from the contribution of all mooring lines and will be discussed in section IV. We will discuss the rest of the terms of this equation separately below.

$$f_i = F_i^{Waves} + F_i^{Lines} + \rho g V_0 \delta_{i3} - C_{ij}^{Hydrostatic} q_j - \int_0^t K_{ij}\left(t-\tau\right)\dot{q}_j\left(\tau\right)d\tau \tag{5}$$

1. Scattering Problem

The first term in Eq. (5), F_i^{Waves}, represents the total excitation load on the support platform from incident waves and is closely related to the wave elevation, ζ. As background, Airy wave theory describes the kinematics of a single *regular* wave, whose elevation is represented as a sinusoid propagating at a single amplitude and frequency (period) or wavelength. (Airy wave theory also describes how the wave particle velocities and accelerations decay exponentially with depth.) *Irregular* or random waves, representing various sea states, are modeled as the summation or superposition of multiple wave components. The Pierson-Moskowitz wave spectrum is routinely used to describe the statistical properties of fully-developed seas and the JOint North Sea WAve Project (JONSWAP) wave spectrum is routinely used in limited fetch situations, in order to prescribe the peak spectral period, significant wave height, and directional content of a sea state.[30] Expressions for ζ and F_i^{Waves} are given by:

$$\zeta\left(t\right) = \frac{1}{2\pi}\int_{-\infty}^{\infty} W\left(\omega\right)\sqrt{2\pi S_\zeta^{2\text{-}Sided}\left(\omega\right)}e^{-j\omega t}d\omega \tag{6}$$

and

$$F_i^{Waves}(t) = \frac{1}{2\pi}\int_{-\infty}^{\infty} W(\omega)\sqrt{2\pi S_\zeta^{2\text{-}Sided}(\omega)}X_i(\omega,\beta)e^{-j\omega t}d\omega \tag{7}$$

Equations (6) and (7) are inverse Fourier transforms where j is the imaginary number $\sqrt{-1}$. $S_\zeta^{2\text{-}Sided}$ represents the two-sided power spectral density (PSD) of the wave elevation per unit time, or two-sided wave spectrum, which depends on the frequency of the incident waves (ω). $W(\omega)$ represents the Fourier transform of a realization of a White Gaussian Noise (WGN) time series process with unit variance and is used to ensure that the individual wave components have a random phase and that the instantaneous wave elevation is Gaussian distributed with zero mean and a variance equal to $\int_{-\infty}^{\infty} S_\zeta^{2\text{-}Sided}(\omega)d\omega$. The same realization is used in the computation of the wave elevation and in the computation of the incident wave force. $X_i(\omega,\beta)$ is a complex-valued array representing the wave excitation force on the support platform normalized per unit wave amplitude; the imaginary components permit the force to be out of phase with the wave elevation. This force depends on the geometry of the support platform and the frequency and direction of the incident wave, ω and β, respectively and is discussed more in section IIIB. The incident wave propagation heading direction, β, which is zero for waves propagating along the positive X-axis of the inertial frame and positive for positive rotations about the Z-axis, is an input to the model, allowing us to simulate conditions in which the wind and wave directions are not aligned.

Equation (7) for the wave excitation force is very similar to Eq. (6) for the wave elevation—the only difference is the inclusion of the normalized wave excitation force complex transfer function, X_i. This follows directly from linearization of the scattering problem. Superposition of the scattering problem implies (1) that the magnitude of the wave excitation force from a single wave is linearly-proportional to the wave amplitude, and (2) that the wave excitation force from multiple, superimposed waves is the same as the sum of the wave excitation forces produced by each individual wave component. In the limit as the difference between individual wave frequencies approaches zero, this sum is replaced with the integral over all incident wave frequencies, as exemplified by Eq. (7). To minimize the wave excitation forces, the floating support platform should be designed with minimal structure near the free surface.

The wave excitation force given in Eq. (7) is independent of the motion of the support platform. This reveals how the scattering problem has been separated from the radiation problem and clearly demonstrates how the linearization assumptions would be violated if the motions of the support platform were large. It follows that Eq. (6) for the wave elevation is only valid at the mean position of the support platform. For other locations, Eq. (6) can be expanded to:

$$\zeta(t,X,Y) = \frac{1}{2\pi}\int_{-\infty}^{\infty} W(\omega)\sqrt{2\pi S_\zeta^{2\text{-}Sided}(\omega)}e^{-jk(\omega)\left[X\cos(\beta)+Y\sin(\beta)\right]}e^{-j\omega t}d\omega, \tag{8}$$

where (X,Y) are the coordinates in the inertial reference frame of a point on the SWL plane and $k(\omega)$ is the *wavenumber*, which is 2π times the number of waves per unit distance along the wave propagation direction (β). For water of depth h, the wavenumber is correlated to the incident wave frequency (ω) and the gravitational acceleration constant (g) by the implicit *dispersion relationship*[29,30]:

$$k(\omega)\tanh\left[k(\omega)h\right] = \frac{\omega^2}{g}. \tag{9}$$

Since the inverse Fourier transforms require a distinction between positive and negative frequencies, the frequency-dependent terms in these equations have several characteristics that ensure the total wave excitation force on the support platform is a *real* function of time. The requirement for this is that the real components of the integrands be an even function of frequency and the imaginary components of the integrands be an odd function of frequency. Thus, the realization of the WGN process has the property that: $W(-\omega) = W^*(\omega)$, where the * is used to denote the complex conjugate. The normalized wave excitation force has the same property:

$X_i(-\omega,\beta) = X_i^*(\omega,\beta)$. And likewise, we set: $k(-\omega) = -k(\omega)$ to ensure that: $e^{-jk(-\omega)} = \left[e^{-jk(\omega)}\right]^*$. The relationship between the two-sided wave spectrum used in the inverse Fourier transforms, $S_\zeta^{2\text{-}Sided}$, and the one-sided wave spectrums commonly used in ocean engineering (Pierson-Moskowitz, JONSWAP), $S_\zeta^{1\text{-}Sided}$, follow standard practice:

$$S_\zeta^{2\text{-}Sided}(\omega) = \begin{cases} \frac{1}{2} S_\zeta^{1\text{-}Sided}(\omega) & \text{for } \omega \geq 0 \\ \frac{1}{2} S_\zeta^{1\text{-}Sided}(-\omega) & \text{for } \omega < 0 \end{cases}. \tag{10}$$

Equation (10) ensures that the variance of the wave elevation, or area under the PSD curves, is the same for both the one- and two-sided spectrums; that is: $\sigma_\zeta^2 = \int_{-\infty}^{\infty} S_\zeta^{2\text{-}Sided}(\omega)\,d\omega = \int_0^{\infty} S_\zeta^{1\text{-}Sided}(\omega)\,d\omega$.

In our computer model, the inverse Fourier transforms are calculated using computationally-efficient Fast Fourier transform (FFT) routines. The realization of the WGN process is calculated using the Box-Muller method and requires that a seed be specified for the pseudo-random number generator (RNG).

2. Hydrostatics Problem

The third and fourth terms in Eq. (5) combined, represent the load contribution from hydrostatics. Here, ρ is the water density, V_0 is the displaced volume of fluid when the support platform is in its undisplaced position, δ_{i3} is the (i,3) component of the Kronecker-Delta function (i.e., identity matrix), and $C_{ij}^{Hydrostatic}$ is the (i,j) component of the linear hydrostatic restoring matrix from the effects of waterplane area and the COB. The hydrostatic loads are independent of the incident and outgoing waves from the scattering and radiation problems, respectively.

The first of these terms, $\rho g V_0 \delta_{i3}$, represents the buoyancy force from *Archimede's Principle*, that is, it is the vertically upwards force equal to the weight of the displaced fluid when the support platform is in its undisplaced position. This term is only nonzero for the vertical heave displacement DOF of the support platform (DOF $i = 3$) since the COB of the platform is assumed to lie on the centerline of the undeflected tower or z-axis of the platform. (If this were not the case, the cross product of the buoyancy force with the vector position of the COB would produce a hydrostatic moment.) In the field of naval architecture and in the analysis of large offshore oil and gas platforms, the term $\rho g V_0 \delta_{i3}$ is not often found in the equations of motion because it cancels with the weight in air of the floating body and the weight in water of the mooring lines. However, with the location of the COG of the floating wind turbine continually changing as a result of wind turbine flexibility, it is important that we separate out the individual contributions of gravity, namely, wind turbine and support platform weight, weight in water of the mooring lines, and buoyancy. The weights of the wind turbine and support platform are inherent in the f_i of Eq. (3).

The second of the hydrostatic terms, $-C_{ij}^{Hydrostatic} q_j$, represents the change in hydrostatic force and moment due to the effects of waterplane area and the COB as the support platform is displaced. The waterplane area of the support platform when it is in its undisplaced, A_0, affects the hydrostatic load since the displaced volume of the fluid changes with changes in the support platform displacement (q_j). Likewise, the body-fixed vertical location of the COB of the support platform, z_{COB}, affects the hydrostatic load since the vector position of the COB also changes with platform displacement (and since the cross product of the buoyancy force with the vector position of the COB produces a hydrostatic moment). (z_{COB} is, in general, less than zero since the z-axis is directed upward along the centerline of the undeflected tower.) The only nonzero components of $C_{ij}^{Hydrostatic}$ are (3,3), (4,4), (5,5), (3,5), and (5,3) when the body-fixed xz-plane of the submerged portion of the support platform is a plane of symmetry[30]:

$$C_{ij}^{Hydrostatic} = \begin{bmatrix} 0 & 0 & 0 & 0 & 0 & 0 \\ 0 & 0 & 0 & 0 & 0 & 0 \\ 0 & 0 & \rho g A_0 & 0 & -\rho g \iint\limits_{A_0} x dA & 0 \\ 0 & 0 & 0 & \rho g \iint\limits_{A_0} y^2 dA + \rho g V_0 z_{COB} & 0 & 0 \\ 0 & 0 & -\rho g \iint\limits_{A_0} x dA & 0 & \rho g \iint\limits_{A_0} x^2 dA + \rho g V_0 z_{COB} & 0 \\ 0 & 0 & 0 & 0 & 0 & 0 \end{bmatrix}. \tag{11}$$

If the body-fixed *yz*-plane of the submerged portion of the support platform is also a plane of symmetry, then the (*3*,*5*) and (*5*,*3*) components of $C_{ij}^{Hydrostatic}$ are also zero. Equation (11) clearly demonstrates how hydrostatics provides restoring only for roll, pitch, and heave motions; restoring in the other modes of motion must be realized by the mooring system. In classical marine hydrostatics, the effects of body weight are often lumped with the effects of hydrostatics when defining the hydrostatic restoring matrix, for example, when it is defined in terms of metacentric heights.[29,30] However, for the same reason given in the previous paragraph for the term $\rho g V_0 \delta_{i3}$ appearing in the hydrodynamic loading equations, it is important that we separate out the contributions of body weight and hydrostatic restoring; thus, to reiterate, $C_{ij}^{Hydrostatic}$ really is the hydrostatic contribution *solely from waterplane area and the COB*.

3. Radiation Problem

The wave radiation loads include contributions from added mass and damping. Because the radiation problem has been separated from the scattering problem, the wave radiation loads are independent of the incident waves.

In Eq. (4), the impulsive hydrodynamic added mass components, A_{ij}, represent the force mechanism proportional to the acceleration of the support platform in the time domain radiation problem. In particular, the (*i*,*j*) component represents the hydrodynamic force in the direction of DOF *i* resulting from the integration (over the wetted surface of the support platform) of the component of the outgoing wave pressure field induced by, and proportional to, a unit acceleration of the j^{th} DOF of the support platform. Like the inertia mass matrix, the impulsive hydrodynamic added mass matrix is symmetric. Unlike the inertia mass matrix, the impulsive hydrodynamic added mass matrix may contain off-diagonal components that couple modes of motion that cannot be coupled through body inertia.

The final term in Eq. (5), $-\int_0^t K_{ij}(t-\tau)\dot{q}_j(\tau)d\tau$, is a convolution integral representing the load contribution from wave radiation damping and, as will become apparent in section IIIB, also represents an additional contribution from added mass not accounted for in A_{ij}. In this expression, τ is a dummy variable with the same units as the simulation time, *t*, and K_{ij} is the (*i*,*j*) component of the matrix known as the *radiation kernel*. In the radiation problem, the free surface brings about the existence of *memory effects*, denoting that the wave radiation loads *depend on the history of motion* for the support platform.

The meaning of the wave radiation kernel is found by considering a unit impulse in support platform velocity. Specifically, the (*i*,*j*) component of the radiation kernel, $K_{ij}(t)$, represents the hydrodynamic force at time *t* in the direction of DOF *i* due to a unit impulse in velocity at time zero of DOF *j*. Thus, the radiation kernel is commonly referred to as the *impulse response functions* of the radiation problem. An impulse in support platform velocity causes a force at all subsequent time because the resulting outgoing free surface waves induce a pressure field within the fluid domain that persists for as long as the waves radiate away. The convolution integral follows directly from linearization of the radiation problem. Superposition of the radiation problem implies that if the support platform

> experiences a succession of impulses, its response at any time is assumed to be the sum of its responses to the individual impulses, each response being calculated with an appropriate time lag from the instant of the corresponding impulse. These impulses can be considered as occurring closer and closer together, until finally one integrates the responses, rather than summing them.[32]

To minimize the wave radiation loads, the floating support platform should be designed with minimal structure near the free surface and the mooring system should be designed to limit the motion of the support platform. The hydrodynamic added mass matrix and kernel from the radiation problem are discussed more in section IIIB.

B. Comparison to Alternative Hydrodynamic Models

The true linear hydrodynamic loading equations discussed in the previous section are the most applicable in the analysis of floating offshore wind turbines. However, alternative hydrodynamic formulations are routinely used in the offshore industry. The two most common alternative hydrodynamic formulations are the *frequency domain* representation and *Morison's* representation. It is beneficial to compare and contrast the true and alternative formulations because it provides additional insight into the hydrodynamics problem and so we can distinguish our model from others used in offshore wind turbine industry.

1. Frequency Domain Representation

The frequency domain representation is most in-line with how marine hydrodynamics is taught in the classroom and presented in textbooks. For instance, the frequency domain representation is the hydrodynamic formulation most emphasized in Refs. 29 and 30, which are popular textbooks in ocean engineering education. The presentation here summarizes those references.

In the time domain representation of the frequency domain problem, Eq. (4) for the total external load acting on the support platform, $F_i^{Platform}$, is replaced with:

$$F_i^{Platform}\left(t\right) = -A_{ij}\left(\omega\right)\ddot{q}_j + Re\left\{AX_i\left(\omega,\beta\right)e^{j\omega t}\right\} - \left[C_{ij}^{Lines} + C_{ij}^{Hydrostatic}\right]q_j - B_{ij}\left(\omega\right)\dot{q}_j\,, \tag{12}$$

where A is the amplitude of a regular incident wave of frequency ω and direction β, C_{ij}^{Lines} is the (i,j) component of the linear restoring matrix from all mooring lines (discussed in section IV), and $A_{ij}\left(\omega\right)$ and $B_{ij}\left(\omega\right)$ are the (i,j) components of the hydrodynamic added mass and damping matrices, which are *frequency-dependent*. $Re\{\}$ denotes the real value of the argument; the only complex-valued terms in Eq. (12) are the normalized wave excitation force, X_i, and the harmonic exponential, $e^{j\omega t}$.

The frequency domain hydrodynamics problem makes use of the same assumptions used in the true linear hydrodynamic formulation with the added requirement that the *incident wave propagates at a single amplitude, frequency, and direction* (i.e., the incident wave is a regular wave) and that the *platform motions are oscillatory at the same frequency as the incident wave*. To reiterate this point, when Eq. (12) is incorporated in Eq. (3), the resulting differential equations are not true differential equations in the proper sense. This is because the time domain representation of the frequency domain problem is only valid when the platform motions are oscillatory at the same frequency as the incident wave (ω). That is, Eq. (12) is only valid for the steady state situation, and not for transient response analysis. A necessary requirement for the platform motions to oscillate at the same frequency as the incident waves is that all additional loading in the system must be linear in nature and that transient behavior must not be considered. Except under steady state conditions, this prevents us from being able to apply the frequency domain hydrodynamics formulation to the analysis of floating offshore wind turbines since nonlinear characteristics and transient events are important aspects of wind turbines. Nevertheless, this approach has been applied in the preliminary design of several floating offshore wind turbine concepts.[21,22,24]

The solution to the frequency domain problem is generally given in terms of the *Response Amplitude Operator* (RAO), which is the complex-valued amplitude of motion of the support platform normalized per unit wave amplitude. In the frequency domain problem, the support platform's response to irregular waves can only be characterized statistically since the frequency domain representation is not valid for transient analysis.

Just like in the true linear hydrodynamic loading formulation, in the frequency domain representation, the radiation and the scattering problems can be solved *separately*. In the radiation problem, six BVPs are solved independently to find six velocity potentials, one for each mode of motion. By substituting these velocity potentials into the linearized, unsteady form of Bernoulli's equation, the resulting pressures, when integrated over the wetted surface of the support platform, yield the added mass and damping matrices. Similarly in the scattering problem, two BVPs are solved independently to find two velocity potentials, one for the incident wave and one for the diffracted wave, and through application of Bernoulli's equation and surface integration again, one arrives at the normalized wave excitation force.

The formulation of the radiation and scattering BVPs, and hence the resulting hydrodynamic added mass and damping matrices (A_{ij} and B_{ij}) and wave excitation force (X_i), depend on frequency, water depth, sea current, the geometric shape of the support platform, its proximity to the free surface, and its forward speed. Additionally, the wave excitation force depends on the heading direction of the incident waves.

The frequency-dependence of the hydrodynamic added mass and damping matrices is of a different nature than the frequency-dependence of the wave excitation force. The frequency-dependence of the hydrodynamic added mass and damping matrices means that the matrices depend on the frequency of oscillation of the particular mode of motion of the support platform. In contrast, the frequency-dependence of the wave excitation force means that the force depends on the frequency of the incident wave. However, in Eq. (12) both frequencies are identical since the platform is assumed to oscillate at the same frequency as the incident wave.

Analytical solutions for the hydrodynamic added mass and damping matrices and wave excitation force are available for bodies of simple geometry, such as cylinders, spheres, etc. Usually, approximations are employed to find these analytical solutions. If the characteristic length of the body is small relative to the wavelength, for example, *G.I. Taylor's long-wavelength approximation* can be used to simplify the diffraction problem. For instance, Morison's equation (discussed next) uses G.I. Taylor's long-wavelength approximation to simplify the diffraction problem for the case of slender, vertical, surface-piercing cylinders. For bodies with complex geometrical surfaces, like the hull of a ship, numerical panel method techniques are required.

Even though the frequency domain formulation cannot be directly applied to the analysis of floating offshore wind turbines, where nonlinear effects, transient behavior, and irregular sea states are important, the solution to the frequency domain problem is valuable in determining the parameters used in the true linear hydrodynamic loading equations. For instance, the solution to the frequency- (and direction-) dependent wave excitation force, $X_i(\omega,\beta)$, is needed not only in the frequency domain problem, but in the time domain formulation of the total excitation load on the support platform from incident waves in Eq. (7). Equally important is the relationship between $A_{ij}(\omega)$ and $B_{ij}(\omega)$ from the frequency domain problem and A_{ij} and $K_{ij}(t)$ from the true linear hydrodynamic formulation. By forcing a particular mode of motion of the support platform to be sinusoidal in the true linear hydrodynamic formulation, and comparing the resulting expression to the time domain representation of the frequency domain problem, it is shown in Ref. 32 that:

$$A_{ij}(\omega) = A_{ij} - \frac{1}{\omega}\int_0^\infty K_{ij}(t)\sin(\omega t)\,dt \tag{13}$$

and

$$B_{ij}(\omega) = \int_0^\infty K_{ij}(t)\cos(\omega t)\,dt\,. \tag{14}$$

The A_{ij} term on the right hand side of Eq. (13) represents the impulsive hydrodynamic added mass matrix of Eq. (4) in the true linear hydrodynamic formulation. Equation (14) is only valid when there is no sea current or forward speed (as assumed); though not given here, a slightly different expression exists when these effects are important. Since the radiation kernel $K_{ij}(t)$ may be assumed to be of finite energy, application of the Riemann-Lebesgue lemma to Eq. (14) reveals that the infinite frequency limit of $B_{ij}(\omega)$ is zero. Similarly, the infinite frequency limit of Eq. (13) yields:

$$A_{ij} = A_{ij}(\infty)\,. \tag{15}$$

Thus, the appropriate added mass matrix to be used in the true linear hydrodynamic loading equations does not depend on frequency, but is the infinite frequency limit of the frequency-dependent added mass matrix, represented here as $A_{ij}(\infty)$. This limit does, in general, exist for three-dimensional bodies.

Through application of Fourier transform techniques and Eq. (15), Eq. (13) and Eq. (14) can be rearranged to show that:

$$K_{ij}(t) = -\frac{2}{\pi}\int_0^\infty \omega\left[A_{ij}(\omega) - A_{ij}(\infty)\right]\sin(\omega t)\,d\omega \tag{16a}$$

or

$$K_{ij}(t) = \frac{2}{\pi}\int_0^\infty B_{ij}(\omega)\cos(\omega t)\,d\omega. \tag{16b}$$

Again, the last expression is only valid when there is no sea current or forward speed (as assumed); though not given here, a slightly different expression exists when these effects are important. It is seen here that the radiation kernel depends both on added mass and damping. Either of the expressions above may be used to find the radiation kernel to be used in the true linear hydrodynamic loading equations once the solution of the frequency domain radiation problem has been found. The sine transform of Eq. (16a) should be used if the solution accuracy for the frequency-dependent hydrodynamic added mass matrix is greater than the accuracy of the solution for the frequency-dependent hydrodynamic damping matrix. The cosine transform of Eq. (16b) should be used if the solution accuracy for the frequency-dependent hydrodynamic damping matrix is greater than the accuracy of the solution for the frequency-dependent hydrodynamic added mass matrix. If the solution accuracy is the same for both the frequency-dependent hydrodynamic added mass and damping matrices, Eq. (16b) is generally a better choice when the integrals are computed numerically since the accuracy of Eq. (16a) is poor near $t = 0$, where $K_{ij}(0)$ is, in general, not zero (even though $sin(0)$ is). Like the inverse Fourier transforms, in our computer model, these sine and cosine transforms are calculated using computationally-efficient routines.

Since the frequency domain approach is so often employed in analyses in the offshore oil and gas industry, there are many computer codes available that solve the frequency domain problem. For instance, the publicly-available SWIM module[8] of the SML computer package discussed earlier may be used to analytically solve the frequency domain problem for support platforms of simple geometry. For platforms of more complicated geometry, the commercially available WAMIT code[11] may be utilized.

The hydrodynamics formulation in FAST and ADAMS can be used regardless of how the radiation and scattering problems are solved. The frequency-dependent hydrodynamic added mass and damping matrices (A_{ij} and B_{ij}) and wave excitation force (X_i) are simply inputs into the models.

2. Morison's Representation

Morison's representation is widely used in the analysis of fixed-bottom offshore wind turbines.[14,16-20] Though somewhat misapplied, it has also been used in the analysis of floating offshore wind turbines.[13,23] Morison's representation, in conjunction with strip theory, can be used to compute the linear wave loads and nonlinear viscous drag loads in a straightforward manner for *slender, vertical, surface-piercing cylinders that extend to the sea floor*. In hydrodynamic *strip theory*, like in BEM theory for wind turbine aerodynamics, the structure is split into a number of elements or strips, where two-dimensional properties (added mass and damping coefficients in the case of hydrodynamics) are used to determine the overall three-dimensional loading on the structure.[30]

The total external load acting on the support platform, $F_i^{Platform}$ as in Eq. (4), is thus found by integrating over the length of the cylinder, the loads acting on each strip of the cylinder, $dF_i^{Platform}$. In Morison's representation, Eq. (4) for the surge and sway modes of motion ($i = 1$ and 2) is replaced with *Morison's equation*[30]:

$$dF_i^{Platform}(t) = -C_A\rho\left(\frac{\pi D^2}{4}dz\right)\ddot{q}_i + (1+C_A)\rho\left(\frac{\pi D^2}{4}dz\right)a_i(t) + \underbrace{\frac{1}{2}C_D\rho(Ddz)\left[v_i(t)-\dot{q}_i\right]\left|v(t)-\dot{q}\right|}_{dF_i^{Viscous}(t)}, \tag{17}$$

where D is the diameter of the cylinder, dz is the length of the differential element of the cylinder, C_A and C_D are the normalized hydrodynamic added mass and viscous drag coefficients, $dF_i^{Viscous}$ is the viscous drag load acting on the strip of the cylinder, and v_i and a_i are the components of the fluid particle velocity and acceleration in the direction of DOF i (discussed below). || denotes the magnitude of the vector difference of v and $\dot{q}$. The first two terms in parentheses involving D and dz are the displaced volume of fluid for the strip of the cylinder. The last term in parentheses involving D and dz is the frontal area for the strip of the cylinder. Please note that Morison's equation is often written in terms of the normalized mass (inertia) coefficient, C_M, in place of C_A, where: $C_M = 1 + C_A$.

Using strip theory, an expression similar to Eq. (17) can be written for the roll and pitch moments ($i = 4$ and 5). Because a cylinder is axisymmetric, the yaw moment ($i = 6$) is zero. And since Morison's equation is only strictly valid for bottom-mounted cylinders, the heave force ($i = 3$) is also zero.

Consistent with Eq. (8) and Airy wave theory, the fluid particle velocity and acceleration in the direction of DOF i, v_i and a_i, at point (X,Y,Z) in the inertial reference frame (where $Z \le 0$) are:

$$v_1\left(t,X,Y,Z\right)=\frac{cos\left(\beta\right)}{2\pi}\int_{-\infty}^{\infty}W\left(\omega\right)\sqrt{2\pi S_{\zeta}^{2\text{-}Sided}\left(\omega\right)}e^{-jk(\omega)\left[X\,cos(\beta)+Y\,sin(\beta)\right]}\omega\frac{cosh\left[k\left(\omega\right)\left(Z+h\right)\right]}{sinh\left[k\left(\omega\right)h\right]}e^{-j\omega t}d\omega\,, \tag{18a}$$

$$v_2\left(t,X,Y,Z\right)=\frac{sin\left(\beta\right)}{2\pi}\int_{-\infty}^{\infty}W\left(\omega\right)\sqrt{2\pi S_{\zeta}^{2\text{-}Sided}\left(\omega\right)}e^{-jk(\omega)\left[X\,cos(\beta)+Y\,sin(\beta)\right]}\omega\frac{cosh\left[k\left(\omega\right)\left(Z+h\right)\right]}{sinh\left[k\left(\omega\right)h\right]}e^{-j\omega t}d\omega\,, \tag{18b}$$

$$v_3\left(t,X,Y,Z\right)=\frac{j}{2\pi}\int_{-\infty}^{\infty}W\left(\omega\right)\sqrt{2\pi S_{\zeta}^{2\text{-}Sided}\left(\omega\right)}e^{-jk(\omega)\left[X\,cos(\beta)+Y\,sin(\beta)\right]}\omega\frac{sinh\left[k\left(\omega\right)\left(Z+h\right)\right]}{sinh\left[k\left(\omega\right)h\right]}e^{-j\omega t}d\omega\,, \tag{18c}$$

and

$$a_1\left(t,X,Y,Z\right)=\frac{jcos\left(\beta\right)}{2\pi}\int_{-\infty}^{\infty}W\left(\omega\right)\sqrt{2\pi S_{\zeta}^{2\text{-}Sided}\left(\omega\right)}e^{-jk(\omega)\left[X\,cos(\beta)+Y\,sin(\beta)\right]}\omega^2\frac{cosh\left[k\left(\omega\right)\left(Z+h\right)\right]}{sinh\left[k\left(\omega\right)h\right]}e^{-j\omega t}d\omega\,, \tag{19a}$$

$$a_2\left(t,X,Y,Z\right)=\frac{jsin\left(\beta\right)}{2\pi}\int_{-\infty}^{\infty}W\left(\omega\right)\sqrt{2\pi S_{\zeta}^{2\text{-}Sided}\left(\omega\right)}e^{-jk(\omega)\left[X\,cos(\beta)+Y\,sin(\beta)\right]}\omega^2\frac{cosh\left[k\left(\omega\right)\left(Z+h\right)\right]}{sinh\left[k\left(\omega\right)h\right]}e^{-j\omega t}d\omega\,, \tag{19b}$$

$$a_3\left(t,X,Y,Z\right)=\frac{-1}{2\pi}\int_{-\infty}^{\infty}W\left(\omega\right)\sqrt{2\pi S_{\zeta}^{2\text{-}Sided}\left(\omega\right)}e^{-jk(\omega)\left[X\,cos(\beta)+Y\,sin(\beta)\right]}\omega^2\frac{sinh\left[k\left(\omega\right)\left(Z+h\right)\right]}{sinh\left[k\left(\omega\right)h\right]}e^{-j\omega t}d\omega\,. \tag{19c}$$

By comparison of Eq. (17) with the true linear hydrodynamic loading equations, it is seen that Morison's representation assumes that *viscous drag dominates the drag load so that wave radiation damping can be ignored*. This assumption is only a valid assumption if the motions of the cylinder are very small (i.e., the cylinder is bottom-fixed and very rigid). The viscous drag load is not included in the linear hydrodynamic loading equations because the viscous drag load is proportional to the *square* of the relative velocity between the fluid particles and platform. Nevertheless, we do include the viscous drag term from Morison's equation in our hydrodynamics model by using an effective platform diameter (D) and by integrating $dF_i^{Viscous}$ over the draft of the support platform to find the total viscous drag load, $F_i^{Viscous}$. We include this effect because it is relatively easy to add and can be an important source of loading in some situations.

By comparison of Eq. (17) with the true linear hydrodynamic loading equations, it is also seen that Morison's representation ignores off-diagonal terms in the added mass matrix. It may do this because a cylinder is axisymmetric, which ensures that there is no added mass-induced coupling between modes of motion. Morison's representation also takes advantage of G.I. Taylor's long-wavelength approximation to simplify the diffraction problem (i.e., the cylinder must be *slender*), which is how the second term in Eq. (17) for the wave excitation force may be expressed in terms of the normalized added mass coefficient. In the linear hydrodynamics problem, C_A theoretically approaches unity ($C_M = 2$) in the infinite-frequency limit. In practice, C_A (or C_M) and C_D must be empirically determined and are dependent on many factors, including Reynold's number, Keulegan-Carpenter number, surface roughness, etc. The assumptions inherent in Morison's representation explain why it is applicable to the analysis of fixed-bottom monopile designs for offshore wind turbines and why we can't apply Morison's representation to the analysis of general support platforms for floating offshore wind turbines (except for the viscous drag term).

One nice feature of Morison's equation, and strip theory in general, is that the loading is written in terms of the fluid velocity and accelerations directly, as opposed to the velocity potential, which are inherent in the hydrodynamic added mass and damping matrices and wave excitation force of the frequency domain problem. This feature allows Morison's equation and strip theory to take advantage of nonlinear wave kinematics models. Such nonlinear wave theories better account for the mass transport, wave breaking, shoaling, reflection, transmission, and other nonlinear characteristics of real waves. Various forms of nonlinear *Stream Function* wave theory, including Dean's theory, Fenton's theory, and Boussinesq theory, are the most widely used when these characteristics are required.[38] A new nonlinear wave kinematics model that does not require the solution to the nonlinear potential flow free surface BVP has also been developed. This model can be used as input to an extended Morison formulation for the evaluation of the wave loads on slender vertical cylinders in steep and random shallow water waves.[39]

IV. Mooring System Dynamics

Mooring systems are used as a means of *stationkeeping*, holding the support platform against wind, waves, and current. In some support platform designs, such as in the TLP, they are also used as a means of establishing stability. A mooring system is made up of a number of cables that are attached to the floating support platform at fairlead connections with the opposite ends anchored to the seabed. Cables are made up of chain, steel, and/or synthetic fibers and are often a segmented combination of these materials. Restraining forces at the fairleads are established through tension in the mooring lines. This tension is the result of the buoyancy of the support platform, cable weight in water, the elasticity in the cable, and viscous separation effects, and it depends on the geometrical layout of the mooring system. As the fairleads move with the support platform in response to unsteady environmental loading, the restraining forces at the fairleads change with the changing cable tension. Thus, the mooring system has an effective compliance.[30]

If the mooring system compliance were inherently linear, the total load on the support platform from the contribution of all mooring lines would be:

$$F_i^{Lines} = F_i^{Lines,0} - C_{ij}^{Lines} q_j \, , \tag{20}$$

where C_{ij}^{Lines} is the (*i*,*j*) component of the linear restoring matrix from all mooring lines and $F_i^{Lines,0}$ is the i^{th} component of the total mooring line load acting on the support platform in its *undisplaced* position. For catenary mooring lines, $F_i^{Lines,0}$ represents the pretension at the fairleads from the weight of the cable not resting on the seafloor in water, and is zero if the lines are neutrally buoyant. For taut mooring lines, $F_i^{Lines,0}$ is the result of pretension in the mooring lines from excess buoyancy in the tank when the support platform is undisplaced, including the contribution of the weight of the cable in water. C_{ij}^{Lines} is the combined result of the elastic stiffness of the mooring lines and/or the effective geometric stiffness brought about by the weight of the cables in water, depending on the layout of the mooring system.

Of course, in general, the mooring line dynamics are not linear in nature; instead, strong nonlinearities are generally evident in the force-displacement relationship. The mooring dynamics also often include nonlinear hysteresis effects, where energy is dissipated as the fairleads oscillate with the support platform around its mean position.

Because mooring system dynamics is a large field of research in and of itself, we have decided to include mooring system effects into our fully coupled simulation model by simply interfacing the publicly-available LINES module of the SML computer package with FAST and ADAMS. This module accounts for nonlinear inertia, restoring, and viscous separation damping effects, including the elastic response of multi-segment lines and their interaction with the seabed. The model does not account for bending stiffness. More details can be found in Ref. 10.

V. Conclusion

The need for comprehensive simulation tools capable of modeling the fully coupled aeroelastic and hydrodynamic responses of floating offshore wind turbines in the time domain led us to upgrade our FAST and ADAMS codes. The features in the upgrades include support platform kinematics and kinetics, linear hydrodynamic loading, and mooring system dynamics. We leverage the analysis tools employed by the offshore oil and gas industries, including the SML and WAMIT codes in the overall solution.

The integration of computational methodologies from the wind energy and offshore oil and gas industries creates a virtual forest of concepts and formulas. In the previous sections of this paper, we walked through that forest investigating each tree in detail, but sometimes, as the saying goes, "it is hard to see the forest for the trees." To help you see that forest, Fig. 3 draws together the presented information.

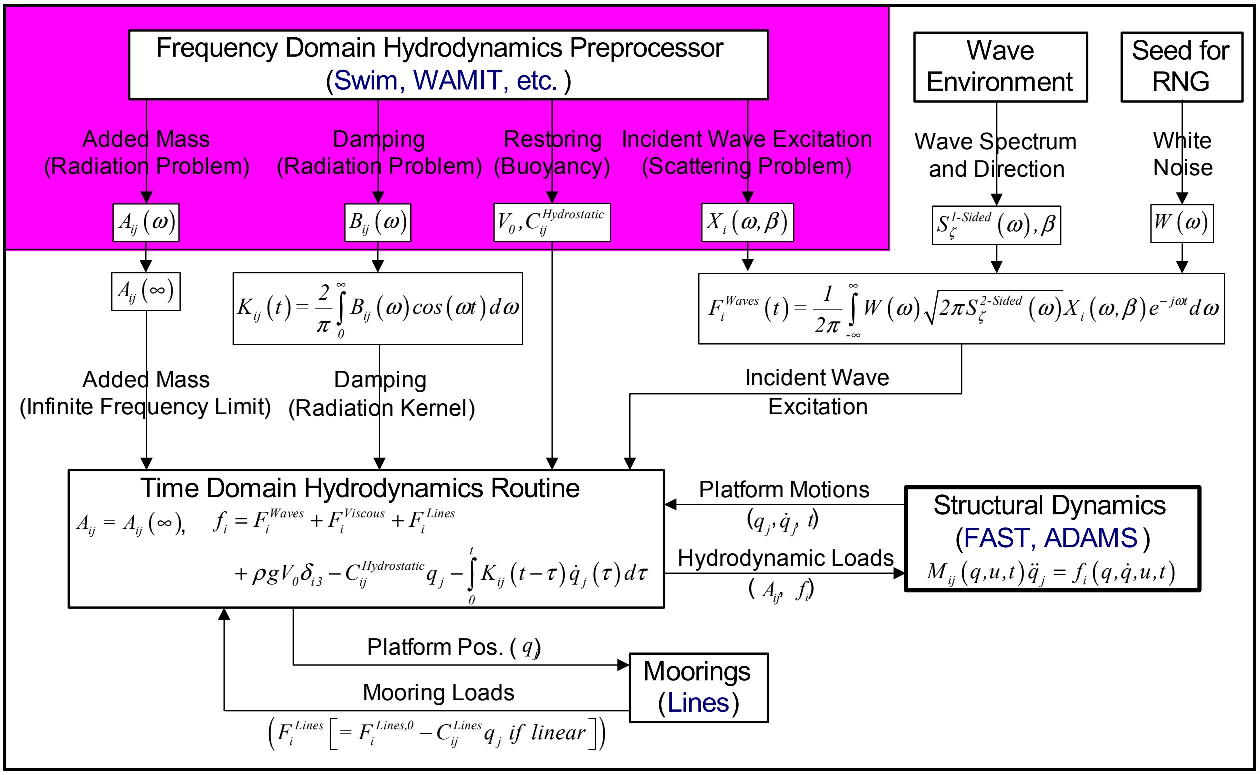

Figure 3. Summary of calculations for the total external load on the support platform.

To summarize, the aeroelastic models of FAST and ADAMS with AeroDyn contain contributions from wind-inflow, aerodynamics, gravity, controls, and the structural dynamics of the wind turbine, including elasticity and the dynamic coupling between the motions of the support platform and the motions of the wind turbine. The loads from the mooring system are obtained by interfacing FAST and ADAMS with LINES and include contributions from inertia, restoring, and viscous separation damping effects, including the elastic response of multi-segment lines and their interaction with the seabed. The hydrodynamic loads on the support platform include the restoring contributions of buoyancy and waterplane area from hydrostatics; the viscous drag contributions from Morison's equation, the added mass and damping contributions from wave radiation, including free surface memory effects; and the incident wave excitation from scattering in regular or irregular seas. The matrices in the hydrodynamic loading expressions depend on the geometry of the support platform and can be found from the solution of the frequency domain problem using SWIM or WAMIT as a preprocessor (represented as the shaded block in Fig. 3). Not included in our model are the effects of sea current, VIV, and loading from sea ice, as well as the nonlinear effects of slow-drift and sum-frequency excitation and high-order wave kinematics.

This work has culminated with enhanced versions of FAST and ADAMS that should prove to be valuable in the design and analysis of floating offshore wind turbines.

Future Work

Using the simulation capabilities described in this work, we plan to perform loads analyses on a few of the promising floating offshore support platform configurations. The results will help identify critical loads and instabilities brought about, in contrast to onshore wind turbines, by the dynamic couplings between and within the turbine and support platform in the presence of combined wind and wave loading. We will assess the critical loads and instabilities in order to identify the technical and economic feasibility of the various system concepts and to determine areas where advanced controls development can be used to improve the coupled system dynamic response.

Additional code enhancements to improve the simulation of floating offshore wind turbines are possible. We would like to introduce second-order, nonlinear hydrodynamic loading models into the codes, including the effects of slow-drift and sum-frequency excitation, which are necessary for accurate modeling of TLP designs. We would also like to add the effects of sea current, VIV, and loading from sea ice.

This work can also be extended to make FAST and ADAMS capable of modeling the fully coupled aeroelastic and hydrodynamic response of fixed-bottom offshore wind turbines. For monopile support structures in shallow water, nonlinear wave kinematics models and Morison's equation for the wave-induced loading must be introduced. For tripod and space-frame designs in intermediate depths, more sophisticated wave loading models are required. Having a single code capable of modeling a large range of support structures and water depths will allow us to perform conceptual studies that attempt to find the optimal transition depth between fixed-bottom and floating platform support structures.

Though not specific to the modeling of offshore wind turbines, we also plan to add a torsion DOF to the modal representation of the tower in FAST and to extend the modal representation of the blades to include mass and elastic offsets, torsion DOFs, and coupled mode shape properties.

Acknowledgments

We would like to thank everyone who helped with this work or inspired its development; including Erik Withee of the US Navy for initiating the study of floating offshore wind turbines at MIT; Kwang Lee of MIT for continuing in the effort and verifying the output of SWIM; Libby Wayman of MIT for modifying SWIM to output the frequency-dependent solutions of the radiation and scattering problems; Walt Musial and Sandy Butterfield of NREL for leading the offshore wind energy program there; Jason Jonkman's Ph.D. committee members at the University of Colorado at Boulder, the University of Wyoming, NREL, and MIT for evaluating the project; and Kathleen O'Dell and Janie Homan of NREL, for editing this paper to make it much more readable.

This work was performed in support of the U.S. Department of Energy by NREL under contract number DE-AC36-99-GO10337 and by MIT under NREL subcontract number XAM-4-33200-04.

References

[1]Musial, Walt; Butterfield, Sandy; and Boone, Andrew, "Feasibility of Floating Platform Systems for Wind Turbines," *A Collection of the 2004 ASME Wind Energy Symposium Technical Papers Presented at the 42nd AIAA Aerospace Sciences Meeting and Exhibit, 5–7 January 2004, Reno Nevada, USA*, New York: American Institute of Aeronautics and Astronautics, Inc. (AIAA) and American Society of Mechanical Engineers (ASME), January 2004, pp. 476–486, NREL/CP-500-36504.

[2]Watson, Greg, et al, "A Framework for Offshore Wind Energy Development in the United States," *Massachusetts Technology Collaborative (MTC)* [online publication], URL: http://www.mtpc.org/offshore/final_09_20.pdf, [cited 17 November 2005].

[3]Jonkman, Jason M. and Buhl, Marshall L., Jr., "FAST User's Guide," NREL/EL-500-29798, Golden, CO: National Renewable Energy Laboratory, October 2004.

[4]Laino, David J. and Hansen, A. Craig, "User's Guide to the Computer Software Routines AeroDyn Interface for ADAMS®," Salt Lake City, UT: Windward Engineering LLC, Prepared for the National Renewable Energy Laboratory under Subcontract No. TCX-9-29209-01, September 2001.

[5]Elliott, A. S., "Analyzing Rotor Dynamics with a General-Purpose Code," *Mechanical Engineering*, Vol. 112, No. 12, December 1990, pp. 21–25.

[6]Laino, David J. and Hansen, A. Craig, "User's Guide to the Wind Turbine Dynamics Aerodynamics Computer Software AeroDyn," Salt Lake City, UT: Windward Engineering LLC, Prepared for the National Renewable Energy Laboratory under Subcontract No. TCX-9-29209-01, December 2002.

[7]Kim, Sungeun and Sclavounos, Paul D., "Fully Coupled Response Simulations of Theme Offshore Structures in Water Depths of Up to 10,000 Feet," *Proceedings of the Eleventh International Offshore and Polar Engineering Conference, 17–22 June 2001, Stavanger, Norway*, The International Society of Offshore and Polar Engineers, 2001.

[8]Kim, Sungeun, "SWIM 2001: Frequency-Domain Analysis of Offshore Platforms, User Manual," Massachusetts Institute of Technology, Cambridge, Massachusetts, 2004.

[9]Kim, Sungeun, "MOTION 2001: Time-Domain Response Analysis of Offshore Platforms, User Manual," Massachusetts Institute of Technology, Cambridge, Massachusetts, 2004.

[10]Kim, Sungeun, "LINES 2001: Nonlinear Static & Dynamic Analysis of Mooring Line/Riser/Tether Arrays, User Manual," Massachusetts Institute of Technology, Cambridge, Massachusetts, 2004.

[11]Lee, Chang Ho and Newman, John Nicholas, "WAMIT® User Manual, Versions 6.2, 6.2PC, 6.2S, 6.2S-PC," WAMIT, Inc., Chestnut Hill, Massachusetts, 2004.

[12]IEC 61400–3, *Wind Turbines – Part 3: Design Requirements for Offshore Wind Turbines*, International Electrotechnical Commission (IEC), 2005 (to be published).

[13]Fulton, Gordon, et al, "Draft Final Report: Semi-Submersible Platform and Anchor Foundation Systems for Wind Turbine Support," NREL Subcontract No. YAM-4-33200-10, Golden, CO: National Renewable Energy Laboratory, July 2005 (to be published).

[14]Kühn, Martin, "Dynamics and Design Optimization of Offshore Wind Energy Conversion Systems," Ph.D. Dissertation, Wind Energy Research Institute, Delft University of Technology, Delft, The Netherlands, 2001.

[15]Butterfield, Sandy; Musial, Walt; Jonkman, Jason; Sclavounos, Paul; and Wayman, Libby, "Engineering Challenges for Floating Offshore Wind Turbines," *Copenhagen Offshore Wind 2005 Conference and Expedition Proceedings, 25–28 October 2005, Copenhagen, Denmark* (to be published).

[16]Passon, Patrick and Kühn, Martin, "State-of-the-art and Development Needs of Simulation Codes for Offshore Wind Turbines," *Copenhagen Offshore Wind 2005 Conference and Expedition Proceedings, 25–28 October 2005, Copenhagen, Denmark* (to be published).

[17]Bossanyi, E. A., "GH Bladed Theory Manual," Issue No. 12, 282/BR/009, Bristol, United Kingdom: Garrad Hassan and Partners Limited, December 2003.

[18]Cheng, Po Wen, "A Reliability Based Design Methodology for Extreme Responses of Offshore Wind Turbines," Ph.D. Dissertation, Wind Energy Research Institute, Delft University of Technology, Delft, The Netherlands, 2002.

[19]Eecen, P. J., "Wind Waves: Forces Due to Waves on Offshore Wind Turbines," ECN-C--03-097, Petten, The Netherlands: Energy Research Centre of The Netherlands, September 2003.

[20]Veldkamp, H. F. and van der Tempel, J., "Influence of Wave Modeling on the Prediction of Fatigue for Offshore Wind Turbines," *Wind Energy*, Vol. 8, No. 1, January/March 2005, pp. 49–65.

[21]Bulder, B. H., et al, "Study to Feasibility of and Boundary Conditions for Floating Offshore Wind Turbines," Novem 2002-CMC-R43, ECN, MARIN, Lagerway the Windmaster, TNO, TUD, MSC, December 2002.

[22]Henderson, Andrew R. and Patel, Minoo H., "On the Modelling of a Floating Offshore Wind Turbine," *Wind Energy*, Vol. 6, No. 1, February 2003, pp. 53–86.

[23]Withee, John E., "Fully Coupled Dynamic Analysis of a Floating Wind Turbine System," Ph.D. Dissertation, Department of Ocean Engineering, Massachusetts Institute of Technology, Cambridge, Massachusetts, USA, 2004.

[24]Lee, Kwang Hyun, "Responses of Floating Wind Turbines to Wind and Wave Excitation," M.S. Dissertation, Department of Ocean Engineering, Massachusetts Institute of Technology, Cambridge, Massachusetts, USA, January 2005.

[25]Moriarty, Patrick J. and Hansen, A. Craig, "AeroDyn Theory Manual," NREL/EL-500-36881, Golden, CO: National Renewable Energy Laboratory, October 2004.

[26]Greeenwood, Donald, T., *Principles of Dynamics*, 2nd ed., Prentice-Hall, Inc., Englewood Cliffs, New Jersey, USA, 1988, pp. 354–358.

[27]Horn, Roger A. and Johnson, Charles R., *Matrix Analysis*, Cambridge University Press, Cambridge, UK, 1985, pp. 427–455.

[28]Kane, T. R. and Levinson, D. A., *Dynamics: Theory and Applications*, McGraw-Hill Inc., New York, 1985.

[29]Newman, J. N., *Marine Hydrodynamics*, The MIT Press, Cambridge, Massachusetts, USA, 1997.

[30]Faltinsen, O. M., *Sea Loads on Ships and Offshore Structures*, Cambridge University Press, Cambridge, UK, 1990.

[31]Cummins, W. E., "The Impulse Response Function and Ship Motions," *Schiffstechnik*, Vol. 9, October 1962, pp. 101–109.

[32]Ogilvie, T. Francis. "Recent Progress toward the Understanding and Prediction of Ship Motions," *Fifth Symposium on Naval Hydrodynamics*, September, 1964, pp. 3–128.

[33]Emmerhoff, Ole J., "The Slow-Drift Motions of Offshore Structures," Ph.D. Dissertation, Department of Ocean Engineering, Massachusetts Institute of Technology, Cambridge, Massachusetts, 1994.

[34]Strum, Robert D. and Kirk, Donald E., *Contemporary Linear Systems Using MATLAB®*, Brooks/Cole, Pacific Grove, California, USA, 2000, pp. 221–297.

[35]Press, William H.; Teukolsky, Saul, A.; Vetterling, William T.; and Flannery, Brian P., *Numerical Recipes in Fortran: The Art of Scientific Computing*, 2nd ed., Cambridge University Press, Cambridge, UK, 1992, pp. 490–498.

[36]Rubinstein, Reuven Y., *Simulation and the Monte Carlo Method*, John Wiley & Sons, Inc., New York, 1981, pp. 86–91.

[37]Sclavounos, Paul D., "13.022 Surface Waves and Their Interaction with Floating Bodies, Lecture Notes," *Massachusetts Institute of Technology (MIT) OpenCourseWare* [online publication], URL: http://ocw.mit.edu/OcwWeb/Ocean-Engineering/13-022Surface-Waves-and-their-Interaction-With-Floating-BodiesSpring2002/CourseHome/index.htm, [cited 27, September 2005].

[38]Demirbilek, Zeki and Vincent, C. Linwood, "Part II: Coastal Hydrodynamics; Chapter II-1: Water Wave Mechanics," *Coastal Engineering Manual* [online publication], EM 1110-2-1100, URL: http://users.coastal.ufl.edu/~sheppard/eoc6430/Coastal_Engineering_Manual.htm, [cited 22 September 2005].

[39]Sclavounos, Paul D., "Nonlinear Particle Kinematics of Ocean Waves," *Journal of Fluid Mechanics*, Vol. 540, 2005, pp. 133–142.

REPORT DOCUMENTATION PAGE

Form Approved
OMB No. 0704-0188

1. REPORT DATE *(DD-MM-YYYY)*
January 2006

2. REPORT TYPE
Conference Paper

3. DATES COVERED *(From - To)*

4. TITLE AND SUBTITLE
Development of Fully Coupled Aeroelastic and Hydrodynamic Models for Offshore Wind Turbines: Preprint

5a. CONTRACT NUMBER
DE-AC36-99-GO10337

5b. GRANT NUMBER

5c. PROGRAM ELEMENT NUMBER

6. AUTHOR(S)
J. Jonkman and P.D. Sclavounos

5d. PROJECT NUMBER
NREL/CP-500-39066

5e. TASK NUMBER
WER6.3101

5f. WORK UNIT NUMBER

7. PERFORMING ORGANIZATION NAME(S) AND ADDRESS(ES)
National Renewable Energy Laboratory
1617 Cole Blvd.
Golden, CO 80401-3393

8. PERFORMING ORGANIZATION REPORT NUMBER
NREL/CP-500-39066

9. SPONSORING/MONITORING AGENCY NAME(S) AND ADDRESS(ES)

10. SPONSOR/MONITOR'S ACRONYM(S)
NREL

11. SPONSORING/MONITORING AGENCY REPORT NUMBER

12. DISTRIBUTION AVAILABILITY STATEMENT
National Technical Information Service
U.S. Department of Commerce
5285 Port Royal Road
Springfield, VA 22161

13. SUPPLEMENTARY NOTES

14. ABSTRACT *(Maximum 200 Words)*
Aeroelastic simulation tools are routinely used to design and analyze onshore wind turbines, in order to obtain cost effective machines that achieve favorable performance while maintaining structural integrity. These tools employ sophisticated models of wind-inflow; aerodynamic, gravitational, and inertial loading of the rotor, nacelle, and tower; elastic effects within and between components; and mechanical actuation and electrical responses of the generator and of control and protection systems. For offshore wind turbines, additional models of the hydrodynamic loading in regular and irregular seas, the dynamic coupling between the support platform motions and wind turbine motions, and the dynamic characterization of mooring systems for compliant floating platforms are also important. Hydrodynamic loading includes contributions from hydrostatics, wave radiation, and wave scattering, including free surface memory effects. The integration of all of these models into comprehensive simulation tools, capable of modeling the fully coupled aeroelastic and hydrodynamic responses of floating offshore wind turbines, is presented.

15. SUBJECT TERMS
offshore wind turbine design modeling; wind turbine simulation; hydrodynamic loading

16. SECURITY CLASSIFICATION OF: a. REPORT	b. ABSTRACT	c. THIS PAGE	17. LIMITATION OF ABSTRACT	18. NUMBER OF PAGES	19a. NAME OF RESPONSIBLE PERSON
Unclassified	Unclassified	Unclassified	UL		19b. TELEPHONE NUMBER (*Include area code*)

Standard Form 298 (Rev. 8/98)
Prescribed by ANSI Std. Z39.18

F1147-E(12/2004)